Journal of Colloid and Interface Science 444 (2015) 115–122

Contents lists available at ScienceDirect

Journal of Colloid and Interface Science

www.elsevier.com/locate/jcis

New insights on the structure of the picloram–montmorillonite surface complexes

Jose L. Marco-Brown [a], María Alcira Trinelli [a], Eric M. Gaigneaux [b], Rosa M. Torres Sánchez [c], María dos Santos Afonso [a,*]

[a] Departamento de Química Inorgánica, Analítica y Química Física e INQUIMAE, FCEN, UBA, Ciudad Universitaria, Pabellón II, C1428EHA Buenos Aires, Argentina
[b] Université Catholique de Louvain, Institute of Condensed Matter and Nanosciences (IMCN), Division Solids, Molecules and Reactivity (MOST), Croix du Sud 2/L7.05.17, B-1348 Louvain-la-Neuve, Belgium
[c] CETMIC (Centro de Tecnología en Minerales y Cerámica), Camino Centenario y 506 CC (49) (B1897ZCA) M. B. Gonnet, Argentina

GRAPHICAL ABSTRACT

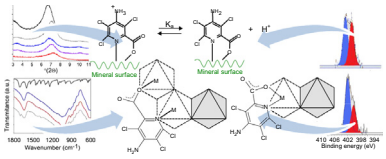

ARTICLE INFO

Article history:
Received 30 August 2014
Accepted 11 December 2014
Available online 26 December 2014

Keywords:
Picloram herbicide
Montmorillonite
Surface complexes
Clay minerals

ABSTRACT

Hypothesis: The environmental mobility and bioavailability of Picloram (PCM) are determined by the amine and carboxylate chemical groups interaction with the soils mineral phases. Clay particles, such as montmorillonite (Mt), and the pH value of the media could play an important role in adsorption processes. Thus, the study of the role of soil components other than organic matter deserves further investigation for a more accurate assessment of the risk of groundwater contamination.
Experiments: Samples with PCM adsorbed on Mt dispersions were prepared at pH 3–9. Subsequently, the dispersions were separated, washed, centrifuged and stored at room temperature. Picloram (PCM) herbicide interaction with surface groups of montmorillonite (Mt) was studied using XRD, DTA, FTIR and XPS techniques.
Findings: The entrance of PCM into the Mt basal space, in two different arrangements, perpendicular and planar, is proposed and the final arrangement depends on PCM concentration. The interaction of PCM with Mt surface sites through the nitrogen of the pyridine ring and carboxylic group of PCM, forming bidentate and bridge inner-sphere complexes was confirmed by FTIR and XPS analysis. The acidity constant of the PCM adsorbed on the Mt surface was calculated.

1. Introduction

The behavior of pesticides in the environment is a dynamic phenomenon. After application, they can reach streams, rivers [1] and lakes, or leach through soil with the possibility to contaminate subsurface waters [2,3]. Hence, better knowledge of the processes controlling the behavior of pesticides in soils for the protection of aquifers and streams is needed [4]. The adsorption of pesticides

Abbreviations: CEC, cation exchange capacity; DTA, differential thermogravimetric analyses; FTIR, Fourier-transform infrared spectra; G–L, Gaussian–Lorentzian; rh, relative humidity; S_{N2}, external specific surface area determined by nitrogen adsorption; XPS, X-ray photoelectron spectroscopy; XRD, X-ray diffraction analysis.

* Corresponding author. Fax: + 54 11 4576 3341.
E-mail address: dosantos@qi.fcen.uba.ar (M. dos Santos Afonso).

http://dx.doi.org/10.1016/j.jcis.2014.12.045
0021-9797/

by soil components is a key process to determine the availability of toxic substances in the soil and their transport to surface and groundwater [5].

Picloram, 4-amino-3,5,6-trichloropyridine-2-carboxylic acid (PCM), is a synthetic organic chemical belonging to the pyridine family of herbicides and also classified as a chlorinated derivative of picolinic acid. Pesticide activity is reported as a systematic herbicide that regulates plant growth. It is used to control annual broadleaf weeds at low rates and deeply rooted herbaceous weeds, vines and woody plants at higher rates in cereals such as wheat, barley, sugarcane and oats [1,6,7]. PCM had been detected in fresh water in a concentration range between 0.3 μg/L [1] and 437 μg/L [8]. The maximum level of picloram contamination in drinking water, recommended by EPA (Environmental Protection Agency, USA), is 0.5 mg/L. Concern about the environment and human health generated the need to seek adsorbents to diminish the concentration of PCM in fresh water and understand the interactions involved.

PCM has an anionic character at the environmental pH of most soils and water ($pK_a \approx 2.3$), which induces very low sorption on soil particles, especially on mineral clays. As a consequence PCM has extremely high soil mobility and was classified as a pesticide with a high leaching potential [9–13]. Basic amine centers and carboxylate groups of the PCM molecule are the responsible groups for the molecule interaction with the adsorbent surface active sites.

The contribution of mineral phases to the availability of pesticides in soils is often considered unimportant and overlooked [14]. Organic matter (OM) has been recognized as the main soil adsorbent but, adsorption on OM cannot always completely explain the pesticide retention in soils. Indeed, chemical groups in the surface of clay particles and the pH value of the media could play an important role in adsorption processes [15]. Then, the study of the role of soil components other than organic matter deserves further investigation for a more accurate assessment of the risk of groundwater contamination.

Soils with different organic matter and clay mineral contents have thus been used to adsorb PCM and a direct relationship between PCM adsorption and organic matter content has been found [11,16,17]. Adsorption of PCM by clays has been reported in very acidic condition [11], while for pH values above 3, PCM adsorption has not been detected [9].

The high cationic exchange capacity and specific surface area of montmorillonite allowed it to be used as target clay mineral to evaluate the sorption of pesticides [18–20] or amino acids [21]. The cationic pesticides thiabendazole and benzimidazole have been proven to highly adsorb on montmorillonite [22,23], while adsorption of a zwitterion such as glyphosate has also been evaluated on montmorillonite and its thermally treated form [24,25].

In previous work [26] it was found that interactions of PCM with clay mineral surfaces showed an anionic profile, with the adsorption decreasing when pH increasing, suggesting that the adsorption of PCM anions was coupled with a release of H_2O or OH^- ions. Also, the increase of Γ_{ads} with C_{eq} after an adsorption *plateau* indicated the existence of successive adsorption processes over different active sites [26]. PCM adsorption on montmorillonite showed evidence of a first monolayer formed up to a certain value of C_{eq} similarly to what has been found for glyphosate and zearalenone [25,27], and above this concentration other sites participated in the adsorption process.

The aim of this work is to study the structure of the surface complexes of PCM adsorbed on montmorillonite through the use of different experimental methods to get a better understanding of the fate of PCM on soil that, finally, determine the mobility and bioavailability of the herbicide on the environment.

2. Experimental

2.1. Materials

Analytical picloram (PCM) (Fig. S1) was supplied by SIGMA (purity 100%, solubility in water 430 ppm (1.78×10^{-3} M), $pK_a = 2.3$. [28], Mr = 241.5 g mol^{-1}) and used as received. All other chemical reagents were provided by Merck PA and used without any further purification. Water was purified in a Milli-Q system from Millipore Inc.

Montmorillonite API # 26, Clay Spur Wyoming, was provided by Ward's Natural Science Establishment, Inc., USA. This montmorillonite (labeled Mt) was manually milled in an agate mortar and sieved to a particle size less than 125 μm. The main properties reported in a previous work [26] were: CEC 138 meq/100 g determined by the formaldehyde method [29], purity >98% determined by XRD [30] and isoelectric point at pH = 3.2 (diffusion potential method [31]).

The structural chemical formula including isomorphic substitutions of Mt ($[(Si_{3.94}Al_{0.06})(Al_{1.56}Fe_{0.18}Mg_{0.26})O_{10}(OH)_2]M^+_{0.32}$) were determined from the chemical analysis following the method of Siguin et al. [32].

2.2. Samples preparation

Adsorption of PCM on Mt dispersions was made as indicated in a previous work [26]. Samples were prepared at pH 3–9 using a PCM initial concentration ($C_{0,PCM}$) ranging from 1.7 to 5.0 mM at constant ionic strength of 1.0 mM KCl. The dispersions were shaken and equilibrated for 48 h at room temperature, adjusting pH (3, 5, 7 or 9) with drops of HCl or KOH solutions. The dispersion pH values were kept in ±0.1 units. The $C_{0,PCM}$ maximum concentration used was established by the low solubility of PCM (1.7 mM for pH 3 and 5.0 mM for pH 5, 7 and 9). Subsequently, the dispersions were centrifuged at 17,000 rpm and the pellet obtained was separated from the supernatant solution. The solids were washed with distiller water several times, centrifuged and stored in desiccators over silica gel, at room temperature, for further analysis and labeled, e.g., as PCM–Mt1.7 for a sample prepared from a PCM solution with $C_{0,PCM}$ = 1.7 mM. Control samples, without PCM, were prepared following the same procedure.

Additionally a mechanical sample of Mt and PCM (denoted as MMS) was obtained for comparing purposes by mixing 5.0 g of Mt with 0.036 g of PCM in a mortar.

2.3. Characterization of the adsorbent and adsorption products

Nitrogen adsorption–desorption isotherms were recorded at 77 K using a Micromeritics ASAP 2010 instrument. Sample Mt was degassed for 12 h at 150 °C prior to measurement. The specific surface area was calculated using the BET method. The porosity evaluation was done via Barrett–Joyner–Halenda (BJH) models, from the desorption branch, considering the presence of slit pores. The total pore volume obtained by Gurvitch method was determined from nitrogen adsorption data at relative pressure of 0.95. The specific surface area for Mt sample was: $SN_2 = 27 \pm 5$ m^2/g [26].

The differential thermogravimetric analyses (DTA) were performed on a 35 mg sample in a Shimadzu instrument (DTA-50), from room temperature to 800 °C at a heating rate of 10 °C/min, in N_2 atmosphere.

Semioriented samples were maintained at relative humidity (rh) of 0.47 for 48 h and then analyzed by XRD. The X-ray diffraction patterns ((001) reflection peak), collected from 3° to 13° (2θ), were obtained using a Philips 3020 with Cu Kα, 30 mA and 40 kV, counting time of 10 s/step.

Fourier-transform infrared (FTIR) spectra of PCM, Mt and PCM–Mt samples were recorded in KBr discs on FTIR Nicolet 8700 spectrometer equipped with a DTGS detector, in the 500–4000 cm^{-1} region, with a resolution of 4 cm^{-1}. FTIR spectra were the result of 1024 co-added interferograms.

X-ray photoelectron spectroscopy (XPS) spectra of nitrogen 1s of PCM, Mt, MMS and PCM–Mt samples were obtained on a Kratos Axis spectrometer equipped with a monochromatized aluminum X-ray source (powered at 10 mA and 15 kV) and an eight-channeltron detector. The pressure in the analysis chamber was about 10^{-6} Pa. The angle between the normal to the sample surface and the direction of photoelectron collection was about 0°. The spectra were analyzed with CasaXPS program version 2.3.14. The C—(C, H) component of the C1s peak of carbon was fixed to 284.8 eV to set the binding energy scale. The analysis of signals was done using a Gaussian–Lorentzian function with a percent relation, %G–L, of 70–30. The sample powders were pressed into small stainless steel troughs of inner diameter 4 mm and 0.5 mm depth, mounted on a multi-specimen holder.

3. Results and discussion

Mt presented a type II nitrogen adsorption–desorption isotherms (Fig. S2A) with a type H3 hysteresis associated with low porosity materials formed by sheet agglomerations with slit-shaped pores [33]. The specific surface area obtained by BET was 27 ± 5 m^2/g respectively. The pore volumes obtained by Gurvitch method was 0.04 cm^3/g. The pore diameter size (w_p) distribution (Fig. S2B) were calculated from the desorption branch of isotherms by the BJH method and correspond to the access pore diameter size distribution. Similar results were previously obtained for a natural montmorillonite [34]. The calculated mesopore diameter distribution, correspond to the interparticle spaces generated by plate particles of montmorillonite.

In previous work [26] it was found that interactions of PCM with clay mineral surfaces showed an anionic profile, because adsorption decrease with pH increase, suggesting that the adsorption of PCM anions was coupled with a release of H_2O or OH^- ions. Also, the increase of Γ_{ads} with C_{eq} after an adsorption *plateau* indicated the existence of successive adsorption processes over different active sites [26]. Similarly to what has been found for glyphosate and zearalenone adsorption on montmorillonite [25,27], for PCM a first monolayer formed up to a certain value of C_{eq} and above this concentration other sites participated in the adsorption process. In order to establish the structure of the surface complexes formed during the adsorption process different analytical methods were used.

3.1. Differential thermogravimetric analysis (DTA)

DTA curves for Mt and PCM–Mt1.7 (pH 3) samples are shown in Fig. 1. The bands between 50 and 110 °C are attributed to the loss of water adsorbed on the external surface, the endothermic processes between 110 and 330 °C to the loss of the hydration water of interlayer cations, and the bands over 300 °C to the loss of structural water existing as hydroxyl groups on the mineral surface and edges [35,36].

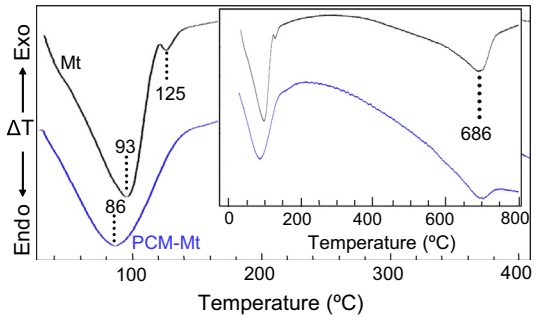

Fig. 1. DTA curves for Mt and PCM–Mt1.7 (pH 3) samples.

Mt sample showed a weight loss at 93 °C, while a shift of 7 °C for PCM-adsorbed sample (t = 86 °C) was observed. Moreover, the endothermic peak at 125 °C corresponding to final dehydration in Mt sample disappeared due to the entrance of PCM into the clay interlayer [37], which favors the removal of hydration water at low temperature (86 °C) as was indicated by Sarbak [38].

The band at 686 °C, in the inset of the Fig. 1, corresponds to the Mt dehydroxylation process and remained after PCM adsorption.

3.2. X-ray diffraction (XRD) analysis

Analysis of (001) reflexion peak revealed an increase of the mineral basal space (from 1.21 to 1.32 nm) for PCM-adsorbed samples with increase of PCM concentration at pH 5, as compared with the untreated sample (Fig. 2). While at pH 7, regardless of the PCM adsorption an interlayer increase of at least 0.04 nm was found.

Experimental and molecular simulation studies on a variety of organoclays showed a linear relationship between the increase of d-spacing and the mass ratio between the organic compound and clay mineral [39]. Considering the disappearance of the endothermic peak at 125 °C and the increase of the (001) reflexion peak would conclude that this is because PCM enters the interlayer.

Moreover, the existence of a second reflection peak is revealed at 2.60 and 2.94 nm with a relative intensity increase with the PCM concentration (Fig. 2), mainly at pH 5, which could be attributed to the molecular rearrangement within the interlayer as was suggested by Zhu et al. [40] for the hexadecyltrimethyl ammonium (CTMA) intercalation on montmorillonite. These authors suggested that the CTMA intercalation continue its rearrangement within the interlayer space during the aging processes [40]. These two types of basal spaces, indicate a heterogeneous interlayer structure generated by the PCM intercalation on Mt.

A molecular model of the PCM protonated molecule was done using HyperChem 8.0.5 software to determine the orientation of the PCM incoming molecule in the interlayer. After applying geometry optimization, the molecule dimensions were approximately estimated (inset in Fig. 2). PCM molecular dimensions were found for deprotonated and zwitterionic molecular shapes. Taking into account the PCM molecular dimensions, the entrance of PCM into

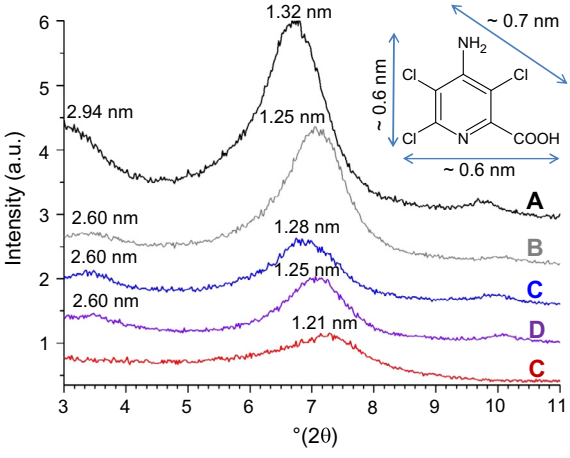

Fig. 2. XRD diffraction patterns of oriented and at rh = 0.47 samples: (A) PCM–Mt5.0, equilibrated at pH 5, (B) PCM–Mt5.0, pH 7, (C) PCM–Mt2.5, pH 5, (D) PCM–Mt2.5, pH 7 and (E) Mt. Inset: protonated PCM molecule dimensions.

the clay interlayer must be in two different arrangements. The first one indicated a PCM perpendicular arrangement respect to the interlayer surface and interacted through pyridine nitrogen and carboxylic groups with the metal centers of the mineral clay surface. For the second one peak, PCM takes a planar arrangement, with water molecule displacement, in agreement with data obtained from the DTA study. Similar results were reported previously for glyphosate adsorption on montmorillonite and its calcined form [24]. These PCM molecular dimensions, are in agreement with those previously found for PCM adsorbed on iron oxide modified Mt [37].

3.3. Fourier-transform infrared (FTIR) spectra

FTIR spectra of PCM, Mt and PCM–Mt samples equilibrated at pH = 5 are shown in Fig. 3A and B, for full spectra and for 600–1800 cm^{-1} regions, respectively. FTIR spectra of PCM–Mt2.5 and PCM–Mt5.0 samples, equilibrated at pH 5, revealed the presence of the herbicide adsorbed on the mineral surface through the presence of bands that belong to PCM, as will be discussed in the paragraphs below.

Two sharp bands appeared in the high frequency region of the FTIR spectrum of PCM, 3474 and 3373 cm^{-1}, corresponding to stretching vibrations of N—H. Most of the characteristic bands related to CH deformation modes and other skeletal vibrations appeared at very similar energies of around 3000 cm^{-1}, where a broad band corresponding to the stretching vibration of hydroxyl ions νOH was also present.

The Mt sample spectrum showed, at 3700 cm^{-1}, a strong broad band corresponding to the stretching vibration of the hydroxyl ions present at the edges of clay platelets or in the mineral bulk between the tetrahedral and octahedral layers, while the broad peak at 3400 cm^{-1} was attributed to the stretching of OH of intercalated water molecules.

PCM coordinated at the surface of the montmorillonite through the pyridine ring nitrogen led to a change of the nitrogen symmetry of PCM–Mt samples with a shift of the stretching vibrations of N—H that cannot be observed due to the presence of the strong and broad absorption band of the stretching vibration of Mt hydroxyl ions.

The band at 1707 cm^{-1} in the PCM spectrum, assigned to carboxyl C=O stretching, shifted to 1700 cm^{-1} in the PCM–Mt5.0 sample spectrum. This band was associated with a protonated carboxylic group and indicated that some PCM was adsorbed in a non-dissociated form [9].

The band at 1602 cm^{-1}, which corresponded to asymmetric stretching vibration ν_a of the dissociated carboxyl group plus the bending vibration of the $-NH_2$ group of PCM, shifted to higher frequencies and overlapped with the mineral band at 1642 cm^{-1}. The shift of the latter band, with two maxima at 1646 and 1636 cm^{-1}, was observed for PCM–Mt2.5 and PCM–Mt5.0 samples indicating that the $-COO^-$ chemical group was involved in surface interactions.

The pyridine-ring vibration ν(C=N) band at 1540 cm^{-1} of the PCM spectrum shifted to 1558 cm^{-1}, indicating the interaction of the pyridine ring nitrogen of the PCM molecule with the mineral clay surface. The band at 1443 cm^{-1}, assigned to the carbon double bond vibration ν(C=C) of the pyridine ring of PCM, appeared as a broad band between 1457 and 1424 cm^{-1} in both PCM–Mt samples due to a shift of the doublet to a higher frequency region. This shift in the absorption frequencies of the ring chemical groups was indicative of a change in the electron density of the ring due to surface coordination by pyridine nitrogen of PCM.

The peak at 1380 cm^{-1} of the PCM spectrum corresponded to symmetric stretching vibration ν_s of the carboxyl group and shifted to 1371 cm^{-1} in PCM–Mt5.0 sample. This shift could be attributed to the interaction of PCM with the solid surface by the formation of a monodentate or bidentate complexes that involves the COO^- and the nitrogen of the pyridine ring groups coordination. Similar results was found for picloram adsorption on pillared montmorillonite [37] indicating that PCM was oriented perpendicular to the external surface and interacted through pyridine nitrogen and carboxylic groups with the metal centers of the mineral clay surface. Also, the PCM coordination on the internal surface centers (silanol groups) was pointed out by the reflection peak shifts that suggest a PCM perpendicular arrangement in the interlayer as was discussed before.

The PCM double band centered at 1295 cm^{-1} due to pyridine δ(CH) was not observed in PCM–Mt samples because it could be overlapped by the broad absorption band of raw Mt in this region. The peak at 1238 cm^{-1} of the PCM spectrum was observed in PCM–Mt5.0 sample as a shoulder corresponding to NH deformation of the herbicide molecule.

The peak at 643 cm^{-1} in PCM spectrum, which was attributed to the $\omega(CO_2^-)$ wagging mode and to the $\delta(CO_2^-)$ bending mode of acid groups [41], moved to 668 cm^{-1} in PCM–Mt5.0 sample suggesting the presence of an interaction of PCM with the Mt surface through the carboxylic group. Similar results were reported for the adsorption of PCM on clay and Al(III), Fe(III) and Cu(II) saturated clays [42]. These authors concluded that the interaction of PCM with mineral surfaces only occurs by the replacement of OH groups from the coordination sphere of copper and further complexation with nitrogen of the pyridine ring.

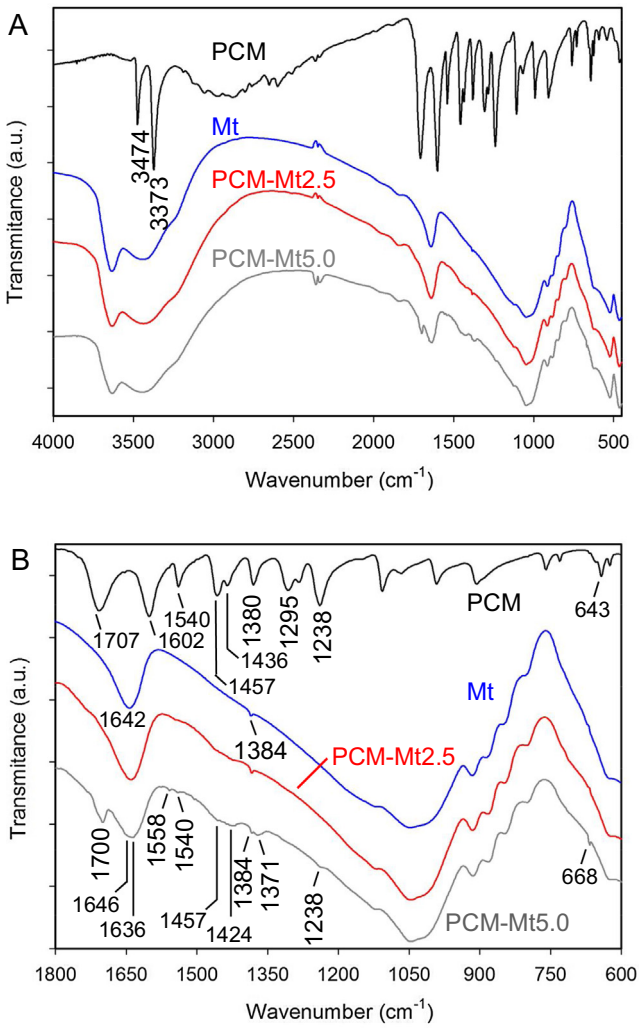

Fig. 3. FTIR spectra at pH = 5 of: (-) PCM, (——) Mt, (——) PCM–Mt2.5 and (——) PCM–Mt5.0. Spectral region A: 500–4000 cm^{-1} and B: 600–1800 cm^{-1}.

3.4. Analysis by X-ray photoelectron spectroscopy (XPS)

The normalized XPS spectrum corresponding to the N1s signal of PCM–Mt1.7 samples equilibrated at the indicated pH values are shown in Fig. 4. The presence of nitrogen on the surface of the samples was solely due to the presence of PCM; the decreasing area of N1s peaks with increasing pH (Fig. 4) can be correlated with PCM adsorption results previously reported [26]. The N1s signals were mathematically decomposed into two components centered at about 403.5 and 400.5 eV, and attributed to protonated (C—$\underline{N}H_3^+$ protonated amine type) and nonprotonated nitrogen (C—$\underline{N}H_2$ amino group type), respectively [43].

For a better understanding of the variation with pH of both N1s signals of PCM–Mt1.7 sample, the resonance structures of PCM are presented in Fig. S3.

The amine lone pair in PCM molecule is associated with the aromatic ring due to the resonance of the PCM molecule; also, the ring chloride substituents are electron attractors, decreasing the amine group capacity to share electrons. Moreover, PCM pyridine nitrogen has two electrons available in a sp^2 orbital that do not participate in the molecule resonance. Therefore the pyridine nitrogen group basicity is higher than that of the amine group [44], and bond formation through the PCM pyridine nitrogen electron pair is more favorable than that through the electron pair of the amine group.

In this sense, the peak at 403.5 eV was attributed to PCM pyridine nitrogen coordinated to the Mt surface which is equivalent to a protonated amine such as C—$\underline{N}H_3^+$. Once PCM was adsorbed, a partial negative-charge transfer from the Mt surface to the molecule ring occurred, allowing the electrons of the amine group to be more available for interaction with protons, i.e., electrons became more basic. The new protonated amine group produced a higher value of bonding energy at 403.5 eV. Moreover, the peak at 400.5 eV was due to PCM pyridine nitrogen, when the PCM molecule did not interact with the clay surface through nitrogen as well as a deprotonated amine group. The proposed structures and their corresponding signals are shown in Fig. 5A and B, corresponding to all PCM interacting with the clay surface and the protonation of a PCM fraction adsorbed, respectively.

To confirm the above suggestions, PCM and Mt mechanically mixed samples (MMS) were analyzed by XPS. The XPS spectrum of N1s signals (Fig. 6A) indicated the absence of PCM interaction through pyridine nitrogen with the clay surface in MMS. Moreover, the N1s spectra of Mt (Fig. 6A) showed the presence of nitrogen, probably due to an external contamination of the samples.

This contamination could correspond to the signal at 403.5 eV for mechanically mixed samples. The absence of PCM interaction through pyridine nitrogen with the surface in these samples generated a similar signal to that obtained for PCM sample (Fig. 6B) with a binding energy of 399.5 eV and corresponding to both nitrogen atoms in the PCM molecule.

The nitrogen molar percentage values in the indicated samples (expressed as # of mol of N_{total}/100 mol of Mt) are listed in Table 1. The N_{total} molar percentages were determined from the N1s signal area in the region between 408 and 396 eV. This area was related to PCM adsorbed on the clay surface and varied about 20% from the coverage obtained from adsorption measurements [26]. Table 1 also shows the percentage area corresponding to C—$\underline{N}H_3^+$ (peak at 403.5 eV) for each sample. An increment of PCM content was observed in all samples with pH decrease, which indicated a higher PCM interaction with the clay surface and a greater amount of PCM molecules with nitrogen of the protonated amine chemical group. This trend is in agreement with the anionic profile in PCM adsorption isotherms reported previously for PCM adsorption on Mt and pillared Mt [26,37].

However, the existence of interactions through the PCM carboxylic group cannot be excluded, as indicated for PCM adsorption on both montmorillonite and iron oxide modified montmorillonite [26,37] or just as found for the adsorption of some acids (acetic, oxalic, citric, benzoic, salicylic and phthalic, etc.) on mineral clays [45,46]. The presence of an interaction through the PCM carboxylic group could not be determined by XPS analysis due to the complexity of the C1s XPS peak originating from the presence of a variety of carbon species.

The adsorption of organic compounds on Mt surface throughout coordination of aluminol and/or silanol groups of the external surface and in the interlayer space was previously suggested [47]. The tendency to form these surface complexes can be compared with

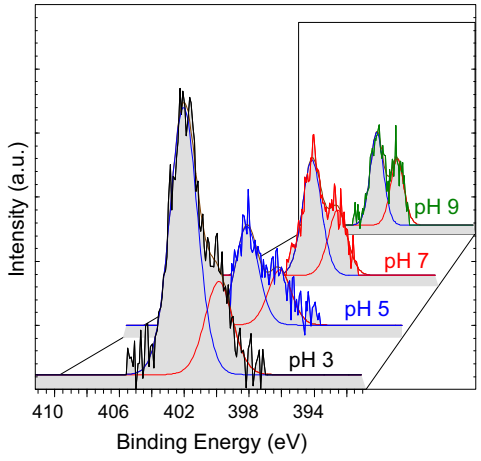

Fig. 4. XPS spectra of N1s signal of PCM–Mt1.7.

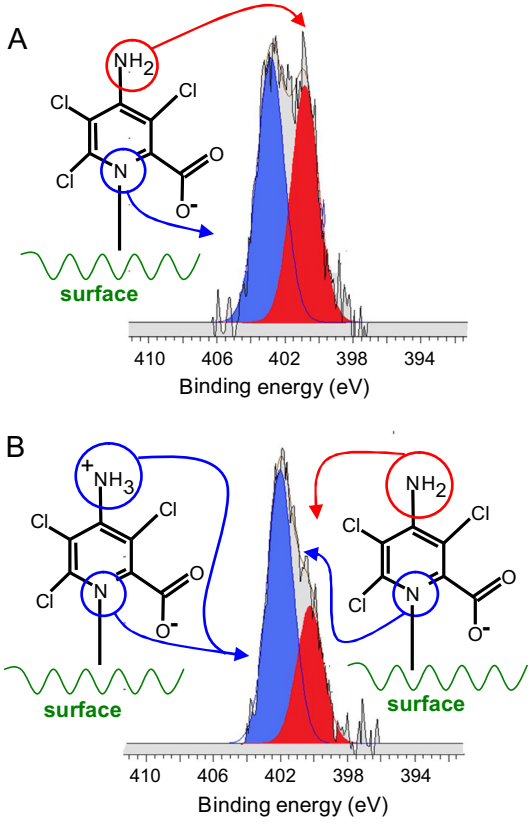

Fig. 5. XPS of N1s signal of PCM–Mt samples.

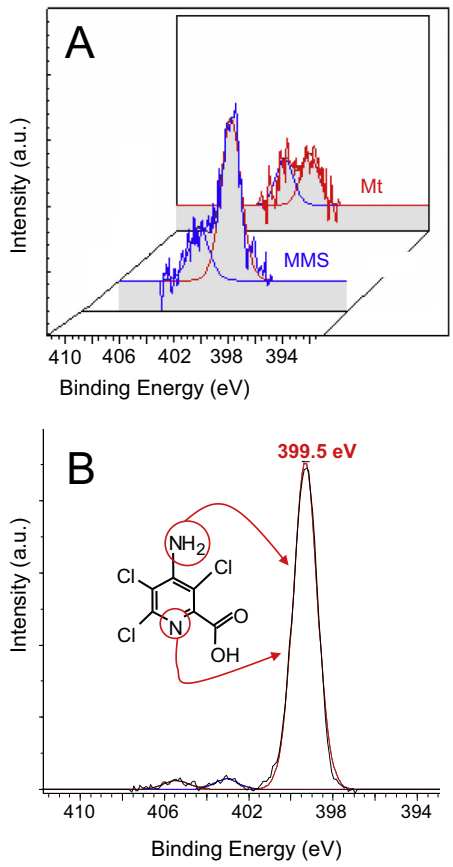

Fig. 6. N1s XPS peak of: (A) MMS and Mt (B) PCM.

Table 1
Molar percentage, determined by XPS, of total nitrogen N_{total} and fraction of the latter present as C—$\underline{N}H_3^+$ species in indicated samples.

Sample	pH	% N_{total}	% C—$\underline{N}H_3^+$
PCM–Mt1.7	3	0.56	74.2
	5	0.34	64.1
	7	0.35	63.8
	9	0.35	58.2
MMS	n.d.	0.46	24.5
Mt	n.d.	0.15	47.6

the tendency to form inner-sphere aqueous complexes [48]. Stable complexes of metals coordinated with pyridine nitrogen and the carboxylate group forming a 5-membered ring was informed for picolinates with silicon and metals such as iron [49] and aluminum [50]. Also, Marco-Brown et al. [37] previously concluded, from FTIR and zeta potential results of PCM adsorbed on pillared clay samples, that the interaction of PCM with the clay mineral surface occurs through the formation of inner-sphere complexes. This metal coordination through pyridine nitrogen and the carboxylate group is in agreement with results obtained by FTIR spectra analysis for the adsorption of picolinic acid on bayerite (Al(III) hydroxide) [41].

A similar behavior can be assumed for the presence of PCM complexes on the clay surface, through coordination of pyridine nitrogen and the carboxylate group to the same surface metal center forming a bidentate complex (Fig. 7A), or through coordination to an adjacent metal center forming a bridge complex as shown in Fig. 7B. Fig. 7A indicates a distance value of 0.28 nm between nitrogen of the pyridine ring and the nearest oxygen of the carboxylate group, determined using HyperChem software. The value obtained was very close to the distance value for two adjacent oxygen atoms of the AlO_6 octahedron (0.27–0.29 nm) of the mineral surface.

The XPS results (Table 1), indicated a C—$\underline{N}H_3^+$ percentage higher than 50, showing that a fraction of the PCM adsorbed had the amino group protonated, as schematized in Fig. 5B.

To explain this behavior, it is important to consider the effect of the mineral clay surface, negatively charged due to isomorphic substitutions, on the electronic environment of PCM. The clay surface coordinated to pyridine nitrogen acts as an electron donor substituent, increasing the negative charge on the heterocyclic ring and decreasing the degree of commitment of the free electrons of the amino group in the PCM molecule. As a consequence of this, the lone electron pair of the nitrogen of the amine chemical group is not shared with the aromatic ring decreasing its contribution to the resonance of the molecule. Therefore, the basicity degree of the amino chemical group increases allowing the formation of the conjugated acid.

Based on this discussion, the acid–base equilibrium shown in Fig. 8 is proposed.

Also, from the discussion above, it could be inferred that the N1s XPS area peak at 403.5 eV could be due to by the contribution of different species:

- Pyridine group of PCM, $\equiv RHN_2$ species coordinated to the surface of clay mineral, whose contribution is equal to the area of the signal at 400.5 eV and equal to the concentration of $\equiv RHN_2$ expressed in area units.
- The pyridine group and protonated amino group of the $\equiv RNH_3^+$ species. Both signals correspond to two different groups of the same molecule whereby the signal is equal to twice the concentration expressed in area units.

Thus, through the value of the N1s XPS areas at 400.5 and 403.5 eV the species concentration at the equilibrium can be estimated according to Eq. (1):

$$A_{403.5eV} = (RNH_2) + 2(RNH_3^+) \quad (1)$$

where $A_{403.5eV}$ is the area of the peak at 403.5 eV and (RNH_2) is the area of the peak at 400.5 eV.

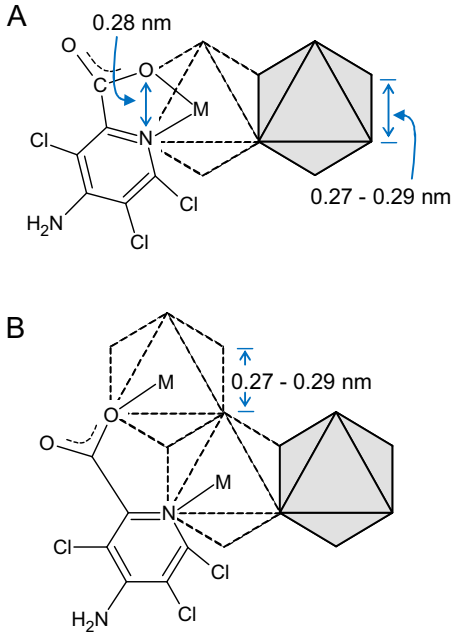

Fig. 7. PCM surface complexes. (A): Bidentate and (B): bridge complexes.

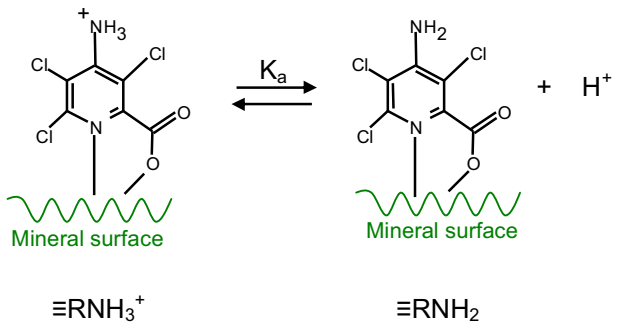

Fig. 8. Equilibrium between $\equiv RNH_3^+$ and $\equiv RHN_2$ species in PCM–Mt samples.

Table 2 lists the (RNH_2) and (RNH_3^+) percent concentration values for PCM–Mt1.7 samples at indicated pH values. The balance proposed in Fig. 8 can be schematically written as:

$$\equiv RNH_3^+ \overset{K_a}{\rightleftharpoons} \equiv RNH_2 + H^+ \quad (2)$$

The acidity constant K_a, corresponding to the deprotonation of the amino group of the PCM adsorbed on the clay surface is expressed as:

$$K_a = \frac{\{\equiv RNH_2\}[H^+]}{\{\equiv RNH_3^+\}} \quad (3)$$

where $\{\equiv RNH_2\}$ and $\{\equiv RNH_3^+\}$ are the concentration of the corresponding surface complexes. By estimating concentrations from Eq. (1), the following equation was obtained:

$$K_a = \frac{\{\equiv RNH_2\}[H^+]}{\{\equiv RNH_3^+\}} = \frac{(RNH_2)[H^+]}{(RNH_3^+)} \quad (4)$$

The K_a value can be calculated as the average of K_a values determined by Eq. (3) for the different pH values, and the $\equiv RNH_2$ and $\equiv RNH_3^+$ species concentration taken from Table 2.

However, for K_a calculation in the analyzed samples, only the values of concentration at pH 3 and 5 were used, because at the more basic pH region, both species, $\equiv RNH_2$ and $\equiv RNH_3^+$ concentrations were very low, which would introduce a substantial error to the calculated K_a value. In addition, it can also be assumed that the concentrations of the $\equiv RNH_3^+$ protonated species at pH 7 and 9 would be small and can be neglected.

Prior to K_a calculation, the percentages of the (RNH_2) and (RNH_3^+) adsorbed species were corrected by a blank subtraction, corresponding to the percentage of the respective species coming from Mt sample contamination.

The pK_a value determined was 3.8 ± 0.8, for the deprotonation of the surface complex for PCM–Mt1.7 sample. This value is in agreement with those found for other pesticides adsorbed onto clay minerals [23,25].

The surface coordinative centers are usually considered as di-, mono- and non-protonated groups. PCM isotherms adsorption previously reported [26] were modeled taking into account the constant values for protonation–deprotonation equilibria [51], the monodentate, bidentate PCM complexes and the deprotonation of the monodentate surface complex that was discussed before.

Table 2
Percent concentrations of $\equiv RNH_2$ and $\equiv RNH_3^+$ surface species on indicated samples.

Sample	pH	(RNH_2)	(RNH_3^+)
PCM–Mt1.7	3	25.8	24.2
	5	35.9	14.1
	7	36.2	13.8
	9	41.8	8.2

Equilibrium constants for the involved reactions are detailed in Table S1 and the experimental results and calculated curves are shown in Fig. S4. The determination coefficients between experimental and theoretical curves were within 0.90–0.95 range which indicate that the proposed model reasonably represents the experimental results.

4. Conclusions

The adsorption pH dependence found in previous work indicated an anionic bonding mechanism of the PCM on the Mt surface. The appearance of an interlayer distance of 2.60–2.94 nm together with PCM adsorption on Mt indicates that the PCM molecule was oriented perpendicular to the interlayer surface and interacted through pyridine nitrogen and carboxylic groups with metal centers of the mineral clay surface. The FTIR and XPS analyses of the PCM–Mt sample suggest inner-sphere complex formation by coordination through the pyridinic/pyridine nitrogen atom and carboxyl group. Moreover, the FTIR and XPS analyses also indicate the formation of bidentate and bridge surface complexes by coordination of one PCM molecule to two external surface sites. Also XPS analysis, by using the concentration of $\equiv RNH_2$ and $\equiv RNH_3^+$ species determined, allowed the calculation of the acidity constant of PCM adsorbed on the Mt surface (pK_a = 3.8 ± 0.8).

Acknowledgments

The authors acknowledge the Universidad de Buenos Aires (UBA) and Ministerio de Ciencia y Tecnología, Agencia Nacional de Promoción Científica y Tecnológica, Fondo para la Investigación Científica y Tecnológica (MINCyT-ANPCyT-FONCyT) for financial support through UBACyT X043, X067, PICT 23-32678 and SECyT/FNRS BE/PA05-EXIII/001 grants. R.M.T.S is member of CONICET and J.L.M-B and M.A.T. acknowledge CONICET fellowships. The authors also are grateful to Michel I. Genet for his assistance with XPS interpretation.

Appendix A. Supplementary material

Supplementary data associated with this article can be found, in the online version, at http://dx.doi.org/10.1016/j.jcis.2014.12.045.

References

[1] G. Palma, A. Sánchez, Y. Olave, F. Encina, R. Palma, R. Barra, Chemosphere 57 (2004) 763, http://dx.doi.org/10.1016/j.chemosphere.2004.08.047.
[2] M. Loewy, V. Kirs, G. Carvajal, A. Venturino, A.M. Pechen De D'Angelo, Sci. Total Environ. 225 (1999) 211, http://dx.doi.org/10.1016/S0048-9697(98)00365-9.
[3] O.P. Bansal, J. Indian Chem. Soc. 88 (2011) 1525.
[4] G.P. Yang, Y.H. Zhao, X.L. Lu, X.C. Gao, Colloids Surf., A: Physicochem. Eng. Aspects 264 (2005) 179, http://dx.doi.org/10.1016/j.colsurfa.2005.05.018.
[5] N. Koleli, A. Demir, H. Arslan, C. Kantar, Colloids Surf., A: Physicochem. Eng. Aspects 301 (2007) 94, http://dx.doi.org/10.1016/j.colsurfa.2006.12.028.
[6] Food and Agriculture Organization of the United Nations FAO, Specifications and evaluations for Agricultural Pesticides, Picloram, 2007. <http://www.fao.org>.
[7] R. Zhang, A.J. Krzyszowska-Waitkus, G.F. Vance, J. Qi, Adv. Environ. Res. 4 (2000) 57.
[8] D.S. Dennis, W.H. Gillespie, R.A. Maxey, R. Shaw, Arch. Environ. Contam. Toxicol. 6 (1977) 421.
[9] R. Celis, M.C. Hermosín, L. Cornejo, M.J. Carrizosa, J. Cornejo, Int. J. Environ. Anal. Chem. 82 (2002) 503, http://dx.doi.org/10.1080/03067310290018785.
[10] M.W. Cheung, J.W. Biggar, J. Agr. Food Chem. 22 (1974) 202.
[11] J.W. Biggar, U. Mingelgrin, M.W. Cheung, J. Agr. Food Chem. 26 (1978) 1306.
[12] R. Celis, M. Real, M.C. Hermosín, J. Cornejo, Eur. J. Soil Sci. 56 (2005) 287, http://dx.doi.org/10.1111/j.1365-2389.2004.00676.x.
[13] M.E. Close, L. Pang, J.P.C. Watt, K.W. Vincent, Geoderma 84 (1998) 45, http://dx.doi.org/10.1016/S0016-7061(97)00120-1.
[14] F. Worrall, A. Parker, J.E. Rae, A.C. Johnson, Eur. J. Soil Sci. 47 (1996) 265.
[15] Z. Li, L. Schulz, C. Ackley, N. Fenske, J. Colloid Interface Sci. 351 (2010) 254, http://dx.doi.org/10.1016/j.jcis.2010.07.034.
[16] R. Grover, Weed Sci. 19 (1971) 417.

[17] W.J. Farmer, Y. Aochi, Proc. Soil Sci. Soc. Am. 38 (1974) 418, http://dx.doi.org/10.2136/sssaj1974.03615995003800030016x.
[18] N. Rauf, S.S. Tahir, J.H. Kang, Y.S. Chang, Chem. Eng. J. 192 (2012) 369, http://dx.doi.org/10.1016/j.cej.2012.03.047.
[19] E. Bojemueller, A. Nennemann, G. Lagaly, Appl. Clay Sci. 18 (2001) 277.
[20] G. Lagaly, Appl. Clay Sci. 18 (2001) 205, http://dx.doi.org/10.1016/S0169-1317(01)00043-6.
[21] N. Kitadai, T. Yokoyama, S. Nakashima, J. Colloid Interface Sci. 338 (2009) 395, http://dx.doi.org/10.1016/j.jcis.2009.06.061.
[22] B. Lombardi, M. Baschini, R.M. Torres Sánchez, Appl. Clay Sci. 24 (2003) 43, http://dx.doi.org/10.1016/j.clay.2003.07.005.
[23] R.M. Torres Sánchez, M.J. Genet, E.M. Gaigneaux, M. dos Santos Afonso, S. Yunes, Appl. Clay Sci. 53 (2011) 366, http://dx.doi.org/10.1016/j.clay.2010.06.026.
[24] M. Damonte, R.M. Torres Sánchez, M. dos Santos Afonso, Appl. Clay Sci. 36 (2007) 86, http://dx.doi.org/10.1016/j.clay.2006.04.015.
[25] G.A. Khoury, T.C. Gehris, L. Tribe, R.M. Torres Sánchez, M. dos Santos Afonso, Appl. Clay Sci. 50 (2010) 167, http://dx.doi.org/10.1016/j.clay.2010.07.018.
[26] J.L. Marco-Brown, M.M. Areco, R.M. Torres Sánchez, M. dos Santos Afonso, Colloids Surf., A: Physicochem. Eng. Aspects 449 (2014) 121, http://dx.doi.org/10.1016/j.colsurfa.2014.02.038.
[27] S.L. Lemke, P.G. Grant, T.D. Phillips, J. Agr. Food Chem. 46 (1998) 3789.
[28] I. Pavlovic, C. Barriga, M.C. Hermosín, J. Cornejo, M.A. Ulibarri, Appl. Clay Sci. 30 (2005) 125, http://dx.doi.org/10.1016/j.clay.2005.04.004.
[29] N.G. Reeve, M.E. Sumner, Soil Sci. Soc. Am. Proc. 35 (1971) 38, http://dx.doi.org/10.2136/sssaj1971.03615995003500010017x.
[30] H. Rietveld, J. Appl. Crystallogr. 2 (1969) 65, http://dx.doi.org/10.1107/S0021889869006558.
[31] M. Tschapek, R.M.T. Sanchez, C. Wasowski, Zeitschrift für Pflanzenernährung und Bodenkunde 152 (1989) 73, http://dx.doi.org/10.1002/jpln.19891520113.
[32] D. Siguín, S. Ferreira, L. Froufe, F. García, J. Mater. Sci. 29 (1994) 4379, http://dx.doi.org/10.1007/BF00414225.
[33] M.S. Ranelovic, M.M. Purenovic, B.Z. Matovic, A.R. Zarubica, M.Z. Momčilovic, J.M. Purenovic, Micropor. Mesopor. Mater. 195 (2014) 67, http://dx.doi.org/10.1016/j.micromeso.2014.03.031.
[34] L. Le Forestier, F. Muller, F. Villieras, M. Pelletier, Appl. Clay Sci. 48 (2010) 18.
[35] W.A. Dick (Ed.), Book Soil Mineralogy Environmental Applications, Soil Science Society of America Inc, Madison, USA, 2002.
[36] B. Caglar, B. Afsin, A. Tabak, E. Eren, Chem. Eng. J. 149 (2009) 242, http://dx.doi.org/10.1016/j.cej.2008.10.028.
[37] J.L. Marco-Brown, C.M. Barbosa-Lema, R.M. Torres Sánchez, R.C. Mercader, M. dos Santos Afonso, Appl. Clay Sci. 58 (2012) 25, http://dx.doi.org/10.1016/j.clay.2012.01.004.
[38] Z. Sarbak, Mater. Chem. Phys. 39 (1994) 91.
[39] D.R. Paul, Q.H. Zeng, A.B. Yu, G.Q. Lu, J. Colloid Interface Sci. 292 (2005) 462, http://dx.doi.org/10.1016/j.jcis.2005.06.024.
[40] J. Zhu, T. Wang, R. Zhu, F. Ge, P. Yuan, H. He, Colloids Surf., A: Physicochem. Eng. Aspects 384 (2011) 401, http://dx.doi.org/10.1016/j.colsurfa.2011.04.023.
[41] A. Trivella, T. Gaillard, R.H. Stote, P. Hellwig, J. Chem. Phys. 132 (2010), http://dx.doi.org/10.1063/1.3356027.
[42] Y. Aochi, W.J. Farmer, Clays Clay Miner. 29 (1981) 191.
[43] P. Canesson, M.I. Cruz, H. Van Damme, in: M.M. Mortland, V.C. Farmer (Eds.), Developments in Sedimentology, Elsevier, 1979, p. 217.
[44] R.T. Morrison, R.N. Boyd, Organic Chemistry, sixth ed., Prentice Hall, New York, 1992.
[45] J.D. Kubicki, L.M. Schroeter, M.J. Itoh, B.N. Nguyen, S.E. Apitz, Geochim. Cosmochim. Acta 63 (1999) 2709, http://dx.doi.org/10.1016/S0016-7037(99)00194-5.
[46] F.P. Bonina, M.L. Giannossi, L. Medici, C. Puglia, V. Summa, F. Tateo, Appl. Clay Sci. 36 (2007) 77, http://dx.doi.org/10.1016/j.clay.2006.07.008.
[47] R.C. Zielke, T.J. Pinnavaia, Clay. Clay Miner. 36 (1988) 403.
[48] W. Stumm, Chemistry of the solid water interface. Processes at the mineral-water and particle–water interface in natural systems, first ed., Wiley & Sons, 1992.
[49] S.L. Jain, P. Bhattacharyya, H.L. Milton, A.M.Z. Slawin, J.D. Woollins, Inorg. Chem. Commun. 7 (2004) 423, http://dx.doi.org/10.1016/j.inoche.2003.12.034.
[50] J.S. Loring, M. Karlsson, W.R. Fawcett, W.H. Casey, Geochim. Cosmochim. Acta 64 (2000) 4115, http://dx.doi.org/10.1016/S0016-7037(00)00499-3.
[51] M.J. Avena, M.M. Mariscal, C.P. De Pauli, Appl. Clay Sci. 24 (2003) 3, http://dx.doi.org/10.1016/j.clay.2003.07.003.